#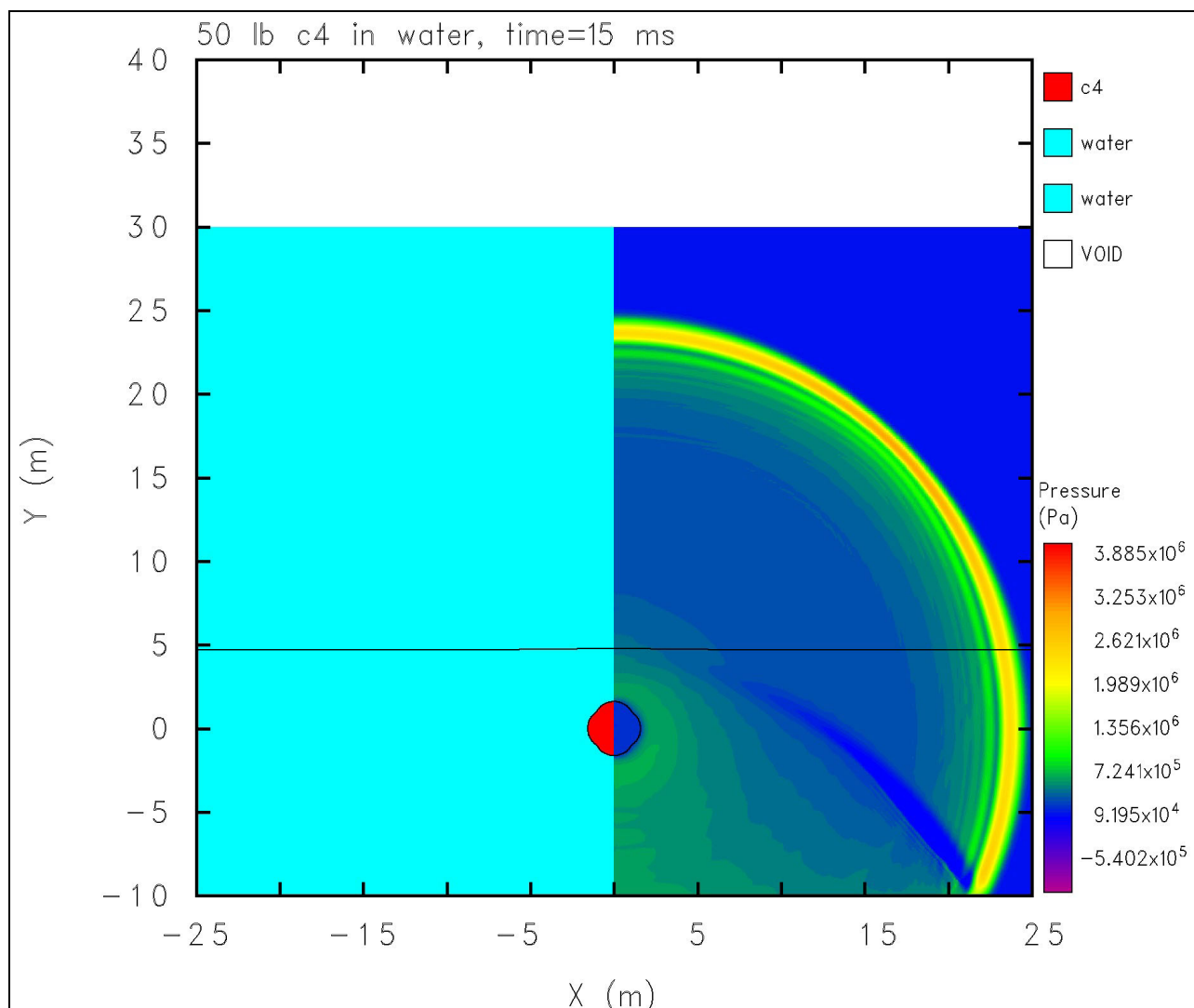 Shock Wave/Sound Propagation Modeling Results for Calculating Marine Protected Species Impact Zones During Explosive Removal of Offshore Structures

U.S. Department of the Interior
Minerals Management Service
Gulf of Mexico OCS Region

Shock Wave/Sound Propagation Modeling Results for Calculating Marine Protected Species Impact Zones During Explosive Removal of Offshore Structures

Prepared by

Peter T. Dzwilewski
Gregg Fenton

Published by

DISCLAIMER

This report was prepared under contract between the Minerals Management Service (MMS) and Applied Research Associates, Inc. This report has been technically reviewed by the MMS, and it has been approved for publication. Approval does not signify that the contents necessarily reflect the views and policies of the MMS, nor does mention of trade names or commercial products constitute endorsement or recommendation for use. It is, however, exempt from review and compliance with the MMS editorial standards.

REPORT AVAILABILITY

Extra copies of this report may be obtained from the Public Information Office (Mail Stop 5034) at the following address:

<div style="text-align:center">

U.S. Department of the Interior
Minerals Management Service
Gulf of Mexico OCS Region
Public Information Office (MS 5034)
1201 Elmwood Park Boulevard
New Orleans, Louisiana 70123-2394

Telephone: (504) 736-2519 or
1-800-200-GULF

</div>

CITATION

ACKNOWLEDGMENTS

TABLE OF CONTENTS

LIST OF FIGURES

LIST OF TABLES

1.0 INTRODUCTION

The explosive removals of offshore structures (EROS) impact marine life. In order to assess that impact adequately, a methodology is needed that accurately models the shock effects caused by the detonation of an explosive charge below the mud line (typically 15 feet) inside a pile, leg, conduit or other structural element. Current methodologies do not take the effects of an explosive detonating below the mud line and the pile leg confinement into consideration in determining shock characteristics in the water at distances. This effort investigated the reduction of energy transmitted to the water resulting from the below-the-mud-line detonation inside a pile or leg. A method was developed that calculates the effectiveness of the explosive as a function of the pile diameter and wall thickness, and the weight of explosive used.

In the sections below, the approach is given (2.0), the literature review is summarized (3.0), the range of parameters is defined (4.0), the calculational matrix is presented (5.0), the results of the baseline and parametric numerical simulations are given (6.0 and 7.0, respectively), the analysis and model development are described (8.0), underwater shock calculational methods are discussed (9.0), the use of the model is demonstrated (10.0), this research work is summarized (11.0) and, lastly, recommendations are given (12.0).

2.0 APPROACH

The approach was to simulate the various pile, explosive, clay, and water conditions numerically with the CTH shock propagation code (McGlaun et al., 1990) to understand the phenomenology of explosive detonations below the sea floor and in offshore structural elements such as piles. From these studies, the effects of explosive burial and pile attributes on the coupling of explosive energy to the water were determined. The end result was that an explosive efficiency factor was defined for each case. For example, if a 50-lb. explosive below the mud line inside of the pile coupled 40% of the energy as a 50-lb. explosive in free water, then the explosive efficiency factor would be 40%. Using the explosive efficiency factor, the user would use 40% of the explosive weight, in this case 20 lb., in calculating the peak pressure, impulse, and energy flux density using free-water equations or other methods.

The steps defined for this approach were:

- ➢ Conduct a literature review to obtain relevant experimental data and studies.
- ➢ Determine the range of parameters that were varied in the numerical simulations.
- ➢ Develop the calculational matrix.
- ➢ Perform the numerical simulations.
- ➢ Analyze the results and develop the models that describe the shock environment (peak pressure, impulse, and energy flux density) in the water.

Each of these steps will be discussed below.

3.0 LITERATURE REVIEW SUMMARY

A literature review was conducted to develop an understanding of the problem, to see what has and is being done in this field, and to help plan the project. The bibliography that was developed is presented in Appendix A.

Underwater blasting is a practice that is well documented in available literature and scientific journals. The mechanical and physical effects of explosive detonation are well known for both the air and water. Shock wave propagation is accurately described by theory and can be understood through the use of shock propagation computer simulation codes such as CTH, as described by McGlaun et al. (1990). In this journal article, the authors describe the intended purpose of computer code and the types of problems that have been examined with this Sandia National Laboratories software tool. A thorough monograph on numerical modeling of explosive detonation can be found in Mader (1979). Mader describes the results of numerical modeling of the detonation process for condensed explosives. Mader's work was performed at Los Alamos National Laboratories over the last three decades. A more conventional and complete treatment of underwater explosions may be found in Cole (1948). Cole provides the fundamentals of underwater shock physics and documents the assumptions and their respective limitations.

Ward et al. (1998) concentrated on sound propagation and attenuation, in particular the modeling of continuous wave and pulse propagation characteristics for different types of sound sources in a range of environments that are typical of the northeast Atlantic. The studies of Ward used techniques from Yelverton et al. (1973) and Swisdak (1978). Yelverton conducted a number of tests to determine the far-field underwater blast effects on mammals and birds using Pentolite-TNT explosive charges up to 8 lbs. at 10 foot depths. Swisdak compiled a large amount of experimental information into one report for the use of creating similitude equations for peak pressure, impulse, time constants, and energy flux density as a function of scaled range for a number of different explosive sources. Range is scaled relative to the weight of the explosive charge. Swisdak's work used the same methodologies as Cole (1948).

Young (1991) conducted experiments that applied shock pressures on various types of fish for developing injury prediction models. These studies showed that cube-root scaling was valid for close-in distances from a charge, but at greater distances the effects of surface rarefaction waves and seabed reflections may play a more dominant role and should be considered when making predictions at large distances.

Goertner (1982) conducted a study to determine the ranges at which sea mammals would be injured by underwater explosions. The purpose was to provide guidance for explosive removal and testing. A computer program was developed under his study that is similar to the type of predictive tool this report describes. The driving equations were based on the scaling of data developed by Yelverton et al. (1973).

This literature review shows the abundance of underwater shock studies for free-water explosions. Much important information was gleaned from this literature review. However, this review shows little work reported on underwater explosions, which included the influence of

explosive detonation below the mud line and pile confinement of explosives. The Connor (1990) study did show a reduction in explosive effectiveness in developing water shock. The measured pressure, impulse, and energy flux density were less than would be expected for a free-water explosion for half-scale experiments and full-scale offshore structure removal operations. The lack of a robust method to account for the actual conditions encountered in off-shore structure removal led us to select a range of parameters for a numerical study that would allow the determination of an effective explosive weight based on the operational environment of the explosive.

4.0 RANGE OF PARAMETERS

Important underwater blasting considerations include, but are not limited to, types of explosives and their properties; energy releases from underwater explosions - amplitude, duration, frequency, pressure, impulse, energy flux density; charge weight and configuration, scaling laws of underwater blasting; details and properties of the structural element to be removed; wave propagation mechanisms - spherical, cylindrical and planar wave propagation; and, measuring equipment and its calibration.

The range of parameters for this study was developed based on the literature and input from MMS staff, as well as Mr. Russell W. Wilcox of DEMEX Explosive Products & Services. These parameters were used as input for the numerical simulations of the near-field explosive effects and subsequent energy coupling to the water.

The major parameters for this study are:

Soil:	Soft clay and stiff Beaumont clay
Explosive Weight:	25, 50, and 100 lbs.
Explosive Type:	C-4 / Cyclotol
Explosive Shape:	Bulk and toroid
Detonation Point:	15 feet below mud line
Pile Material:	Steel
Pile Diameter:	24", 36", 48", and 72"
Pile Wall Thickness:	¾", 1½" and 2½"

5.0 CALCULATIONAL MATRIX

A total of eighteen numeric simulations were performed to quantify the effects of the pile/mud/explosive configuration on the water shock. This selected set of runs was chosen to cover a wide range of typical conditions to facilitate the model development while limiting the number of calculations because of the relatively short duration of this project. A high fidelity numeric simulation is costly in time of setup and execution. Therefore, we chose a select group of simulations that would sufficiently answer our questions. All simulations were computed using a C-4 explosive, which has nearly the same explosive performance as Cyclotol (their explosive release energies are within 2½% of each other). A 15-foot explosive burial depth was used for all numerical simulations.

All the numeric simulations were performed with the CTH Eulerian hydrocode, which was developed at Sandia National Laboratories. This code handles complex one-, two-, and three-dimensional geometries for shock propagation problems, and non-linear material properties. It is a first principle finite difference code that uses conservation of mass, momentum, and energy along with equations-of-state and strength models for the various materials. The geometry and materials are modeled in a discretized grid. For these calculations, the two-dimensional cylindrical (i.e., axisymmetric) grid contained approximately 130,000 cells. The code uses an explicit solver, meaning that it solves the problem for a single time step (that is automatically determined based on shock properties of the simulation to ensure numeric stability) and marches forward in time until the specified end time is reached. The time step ranged from 3 to 8 microseconds, and the typical CTH numerical simulation took 3 to 8 hours on a 1-GHz Linux workstation.

Five numeric simulations were performed for free water or mud (i.e., no pile) as listed in Table 1. These simulations basically show the variation of shock characteristics caused by a bulk charge weight within water at a selected location for measurement. The single soil-only numerical simulation was performed to isolate the effect of the soil on the shock propagation into water.

Table 1. Free-water and Soil Numerical Simulations.

Medium	Explosive Weight, lbs.			
	12.5	25	50	100
Free water	X	X	X	X
Soil			X	

Table 2 shows the thirteen calculations that were done for the pile cases. This set of simulations was run to understand the effects of pile geometry and properties for the various charge weights.

Table 2. Pile Numerical Simulations

Pile Wall Thickness (inches)	Pile Diameter (inches)			
	24	**36**	**48**	**72**
¾	25 lb.			
1½ 1½ 1½ 1½	50 lb.	50, 100 lb. 50 lb (soft clay) 50 lb. (water) 50 lb. (toroid)	100 lb.	100 lb.
2½		50, 100 lb.	100 lb.	100 lb.

To separate the effects of the soil and the pile, one calculation was done without a pile (50 lbs, Table 1) and another calculation was done with a pile but without soil (50 lb., 36" diameter, 1½" wall thickness, Table 2). One calculation was done with a toroidal charge instead of a bulk charge to investigate any differences in energy coupling to the water caused by the explosive charge shape (50 lb., 36" diameter, 1½" wall thickness, Table 2). One calculation was done with the pile in soft clay while the others were done in stiff clay.

6.0 BASELINE NUMERICAL SIMULATIONS

The first four simulations were designated as baseline simulations whose objectives were to gain an understanding of the phenomena and isolate the factors that affect the amount of energy coupled into the water.

The four baseline calculations were:
1. 50-lb. explosive – free water
2. 50-lb. explosive – stiff clay (no pile)
3. 50-lb. explosive – pile and water (no clay)
4. 50-lb. explosive – pile in clay, and water

These near-field calculations extended from the explosive charge to approximately 30 m in each direction. The 30 m distance was chosen to be more than twice (2.3 X) the extent of the strong shock or nonlinear region as cited in Richardson et al. (1995) and Ward et al. (1998). Each calculation was run out to a simulation time of 20 to 25 ms, which is the time it takes for the shock wave to propagate 30 to 37 m through water. The energy coupled to the water was monitored, as well as the pressure, impulse, density, particle velocity, temperature, and other thermodynamic variables at various points in the calculational grid.

The material plots (left) and the pressure fields (right) at a time of 15 ms are shown for the free-water calculation in Figure 1, the clay calculation in Figure 2, the pile in water calculation in Figure 3, and lastly, the pile in clay calculation in Figure 4. The general appearance of the pressure fields for the four baseline calculations is similar, in that the pressure field shows a spherical divergent wave propagating from the detonation point and an explosive cavity forming. The free water case has higher pressures at the shock front than the other cases. The kinetic energy coupled to the water is compared in Figure 5. Here the differences in the four numerical simulations are clearly shown. Note the decrease of the kinetic energy at a time around 20 ms is caused by water passing out of the calculational grid as the boundaries were set as transmitting. The free-water case has the highest energy, while the case with the explosive detonating in clay (no pile) shows about a 20% decrease. The case with the pile in water reveals the kinetic energy to be approximately 50% below that of the free-water case. This demonstrates that the pile has a stronger influence on the water coupling than just the clay. Lastly, kinetic energy for the pile in clay is reduced by approximately 60%.

The explosive coupling efficiencies that were defined by dividing the kinetic energy coupled into the water for each simulation by the kinetic energy for the free water case for the four baseline calculations are shown in Table 3. Interestingly enough, if the efficiency for the clay only case (79%) is multiplied by the efficiency of the pile in water only case (49%), one obtains the efficiency for this combined case of the pile in the clay (39%). The implication is that the effects can be identified, isolated, and quantified.
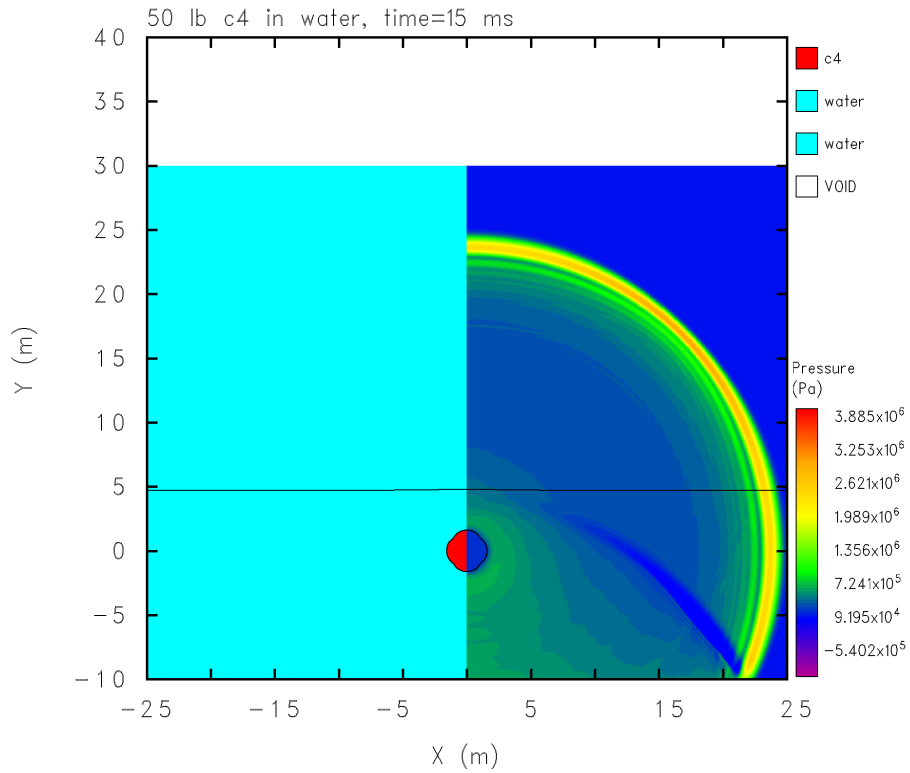
Figure 1. Material and Pressure Field for 50-lb C-4 Free-water Calculation at 15 ms.
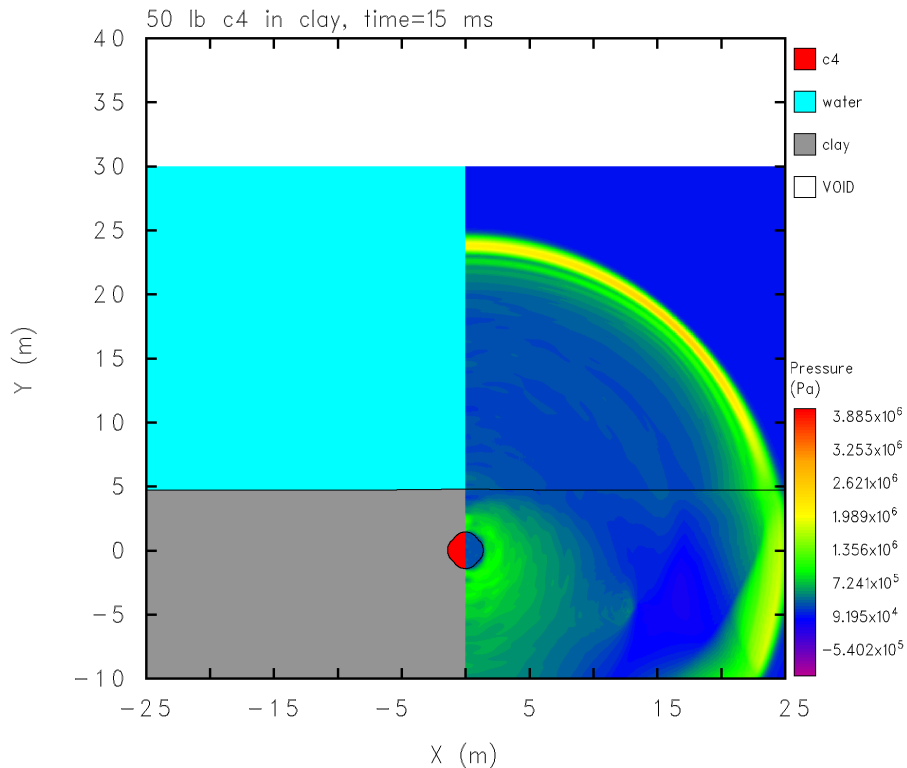
Figure 2. Material and Pressure Field for 50-lb C-4 Free-water Clay Only Calculation at
15 ms.
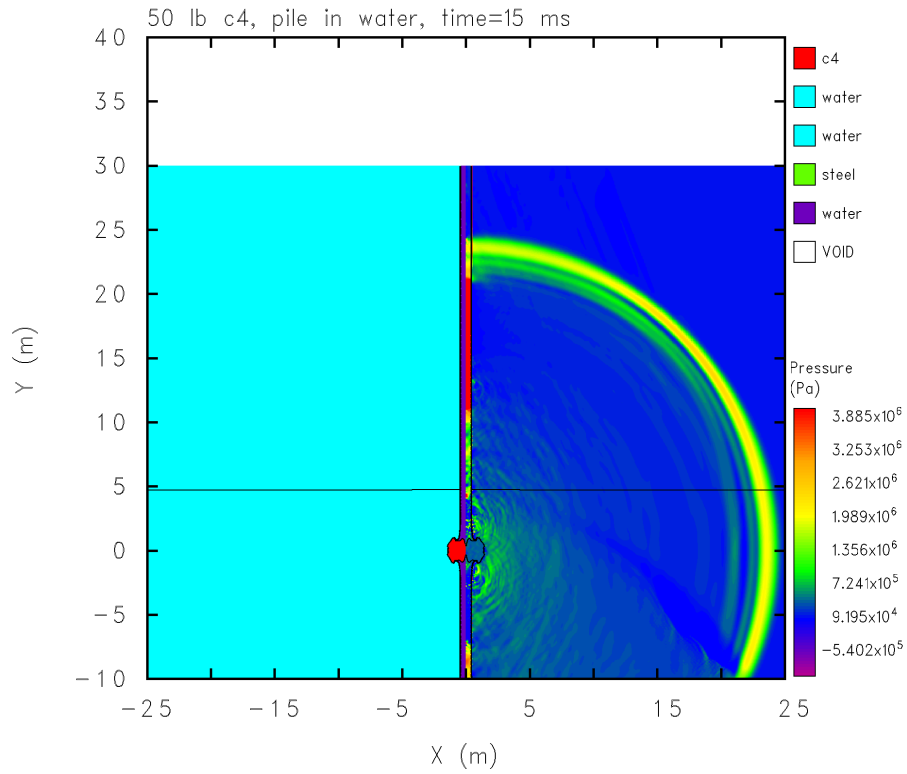
Figure 3. Material and Pressure Field for 50-lb C-4 Pile in Water Calculation at 15 ms.
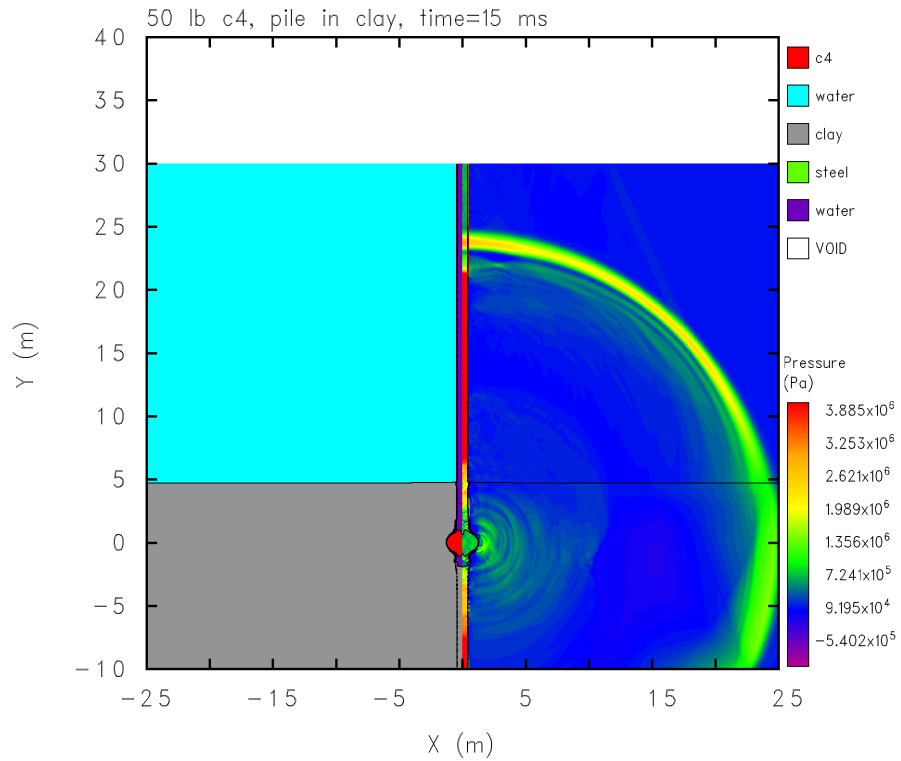
Figure 4. Material and Pressure Field for 50-lb C-4 Pile in Clay Calculation at 15 ms.
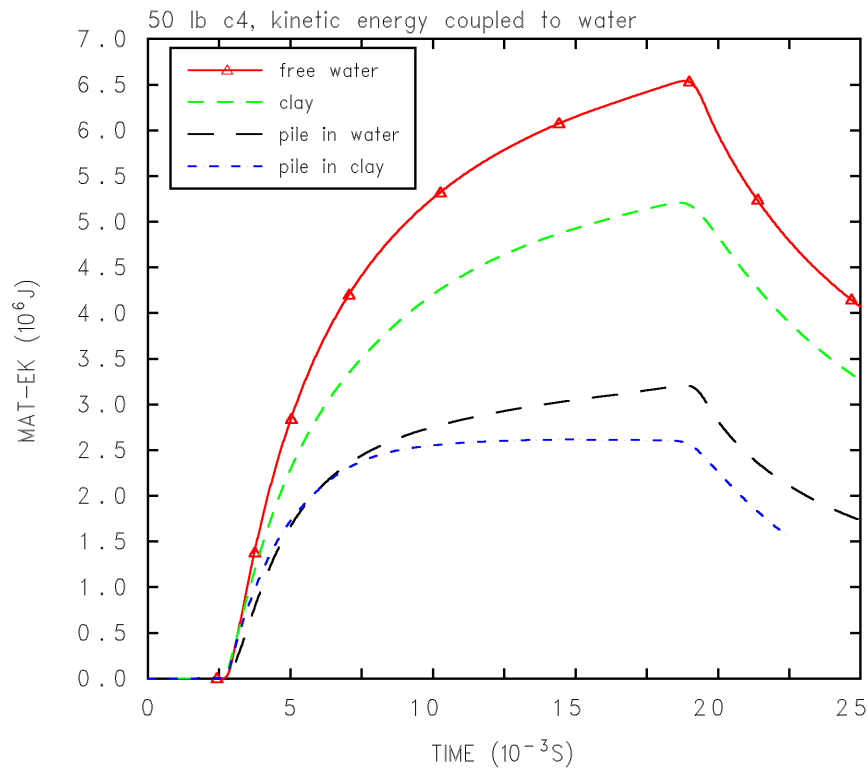
Figure 5. Comparison of Kinetic Energy Coupled into the Water for Baseline Numerical Simulations.

Table 3. Explosive Coupling Efficiencies for the Four Baseline Numerical Simulations – 50-lb. Explosive Weight.

Numerical Simulation	Explosive Coupling Efficiency
Free water	100%
Stiff Clay (no pile)	79%
36" diameter, 1½" wall thickness in water (no clay)	49%
36" diameter, 1½" wall thickness in clay	39%

The pressure and impulse time histories at a range of 20 m are compared with the baseline calculations in Figure 6 and Figure 7, respectively. The pressure waveforms in Figure 6 show that these calculations with confinement caused by clay and/or pile have lower peak pressures than the free water case. More significantly, the pressure drops off faster, as can be more dramatically seen in the impulse comparisons in Figure 7. The clay only calculation shows some reduction in impulse, while the pile in water and pile in clay cases show a very significant reduction in impulse. This drop in impulse is another indication of reduced energy coupling and lower effective explosive weight.

11
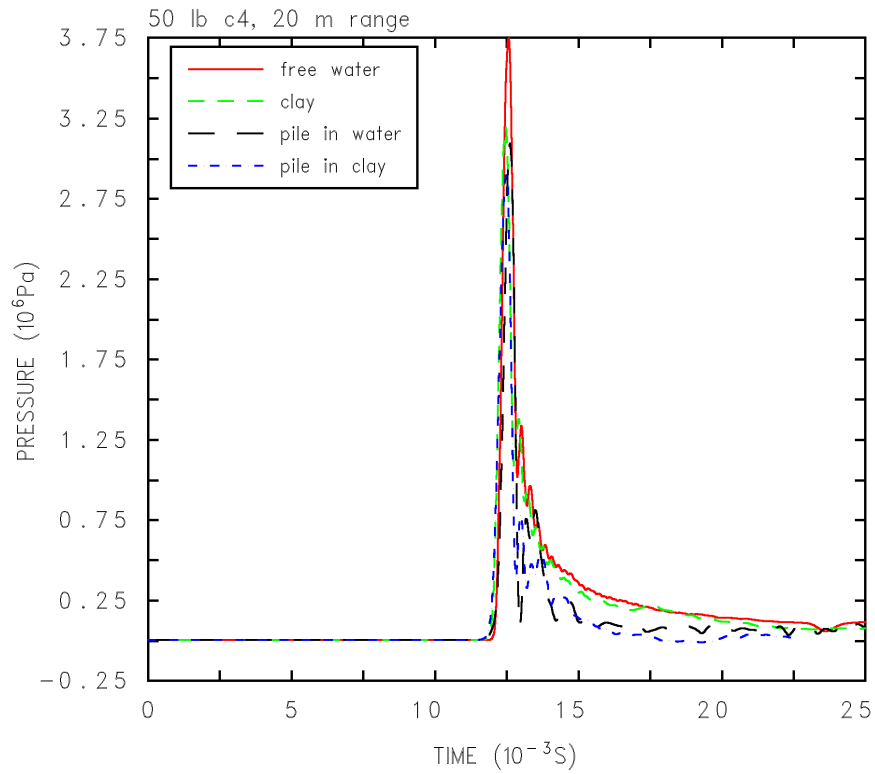
Figure 6. Comparison of Pressure Time Histories at the 20-Meter Range.
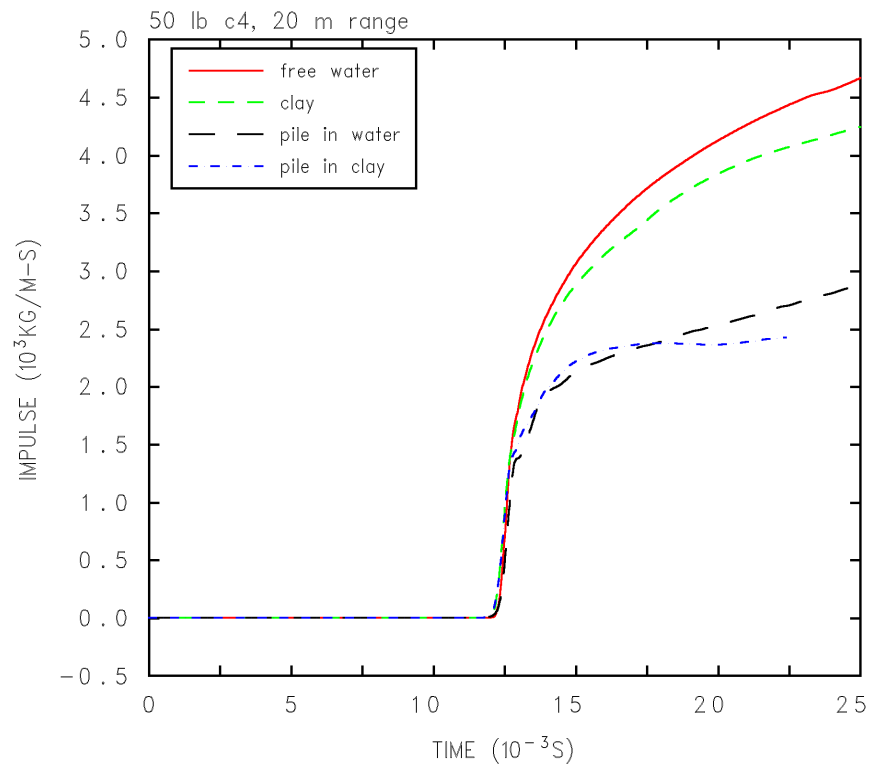
Figure 7. Comparison of Impulse Time Histories at the 20-Meter Range.

12

From Table 3, the pile in clay case has a 40% explosive coupling efficiency, or 60% less energy than the free water case. In order to investigate this finding more, comparisons of this pile in clay simulation were made to 12.5-, 25-, and 50-lb C4 free water calculations. The kinetic energy comparisons are presented in Figure 8, while the pressure and impulse time histories are compared in Figure 9 and Figure 10, respectively. These comparisons support the idea that a pile in clay scenario couples less energy to the water continuum than a free-water explosion and that the reduction in coupled energy is 50% or greater, in this case, being approximately 60%. Put another way, the pile in clay case coupled 40% of the free-water explosion case.

These simulations showed that a reduction of coupled energy into the water was dominated by the pile influence and soil confinement. Both pile and soil confinement offer inertial and strength effects which need to be overcome by the explosive prior to explosive energy deposition into the water. The pile confinement has a greater effect than the soil due to the higher strength and density of the pile material. The numerical simulations also indicate that some energy loss is due to explosive energy propagating in the water inside the pile (typically less than 5%).
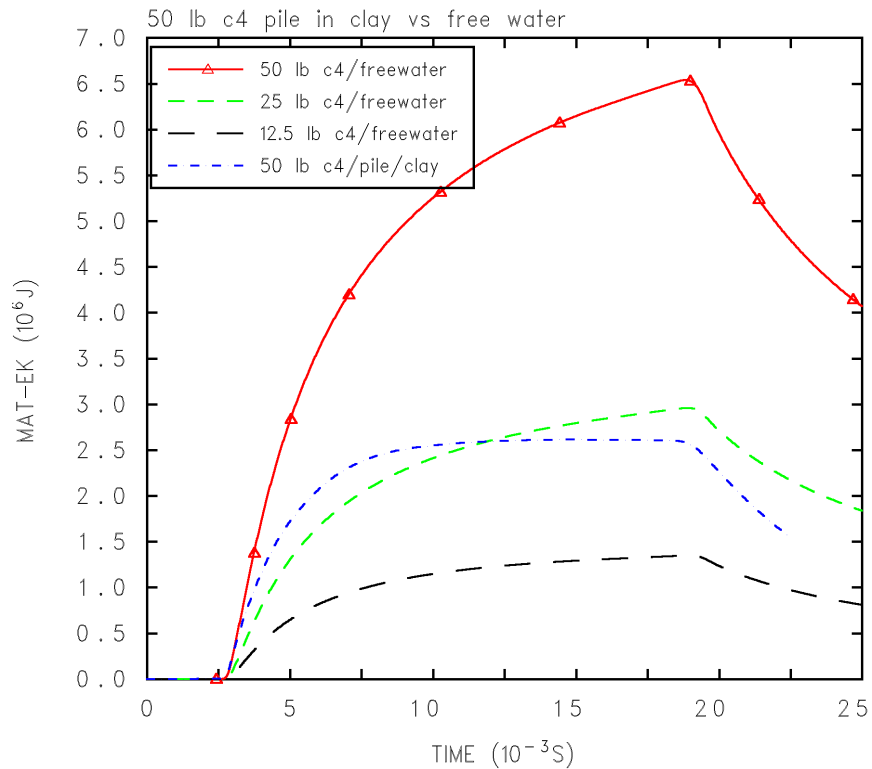
Figure 8. Kinetic Energy Coupled into the Water for Pile in Clay and Free-water Numerical Simulations.
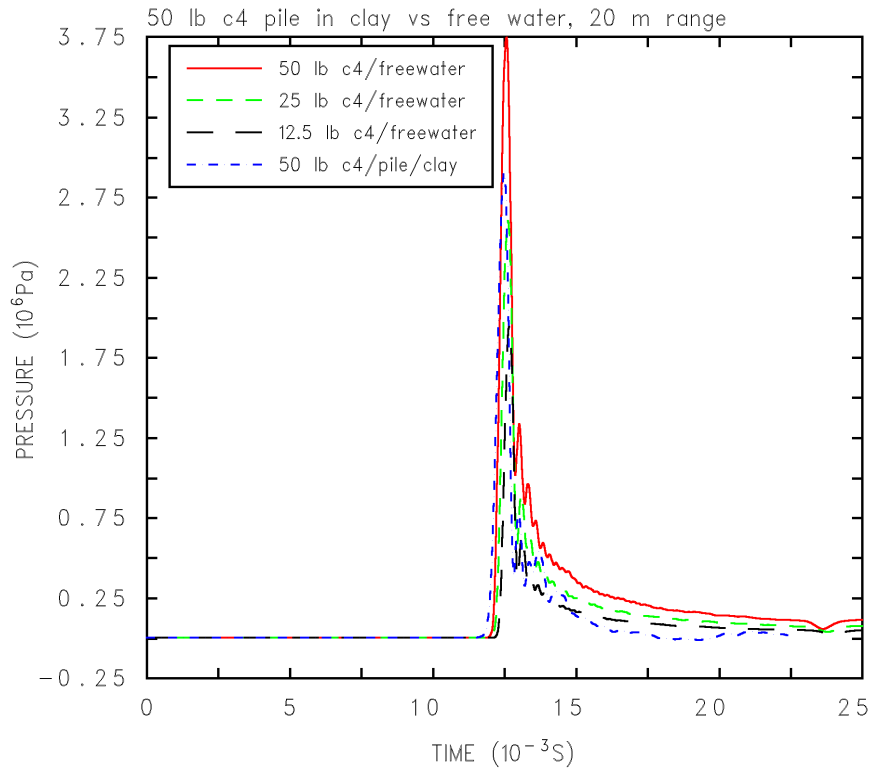
Figure 9. Pressure Time Histories for Pile in Clay and Free-water Numerical
Simulations.
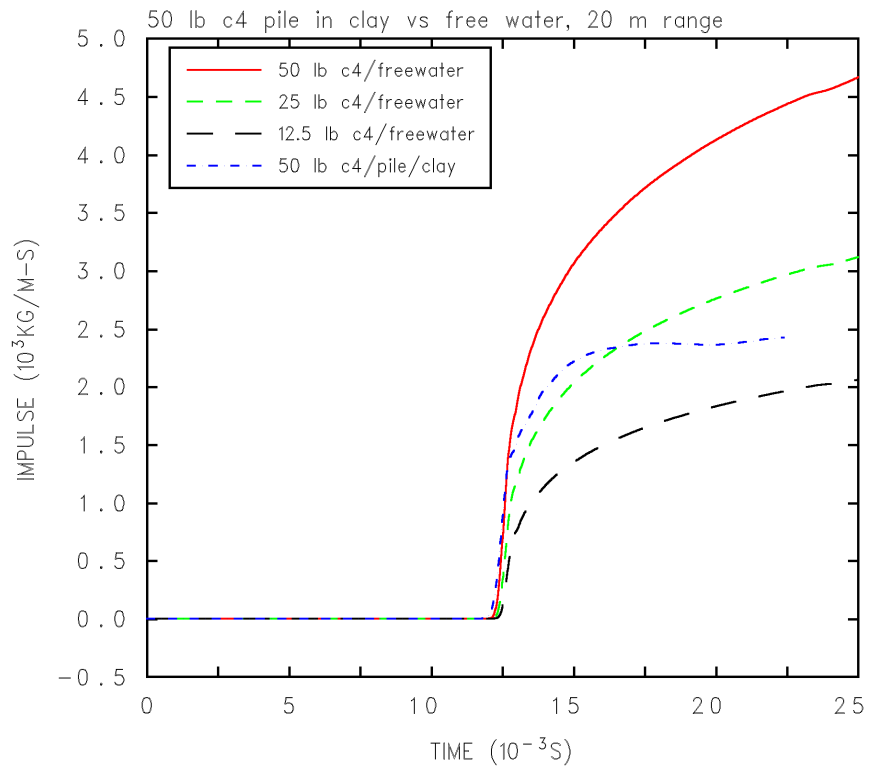
Figure 10. Impulse Time Histories for Pile in Clay and Free-water Simulations.

7.0 PARAMETRIC NUMERICAL SIMULATIONS

To further define the explosive coupling efficiency over a broader range of pile diameter, wall thickness, clay strength, and explosive weight, numerical simulations were performed for the conditions previously given in Table 2. Note this was a parameter study and the explosive amount for a particular pile presented here is not necessarily the optimum or recommended value.

The results of these numerical simulations were analyzed in a similar way to the baseline calculations presented in the previous section. The energy coupling efficiency was calculated by dividing the coupled energy to the water by the appropriate free water value. The resulting energy coupling efficiencies are presented in the parametric variations in Table 4. A 3% difference between the coupling efficiencies of a bulk charge to that of a toroidal charge for the same pile geometry is shown in Table 4. This small difference is caused by the toroidal charge being closer to the pile wall and thus is able to deliver more energy into the surrounding water. Also, the use of a soft clay model which is less dense, more compressible, and had about one-third of the strength of the stiff clay caused a 4% increase in the energy coupling to the water.

Table 4. Explosive Coupling Efficiencies for Pile Geometry in Clay Numerical Simulations.

Pile Wall Thickness (Inches)	Explosive Weight (lb.)	Pile Diameter (Inches)			
		24	36	48	72
¾	25	45%			
1½	50	44%	39%		
	50 (soft clay)		43%		
	50 (toroid)		41%		
	100		48%	51%	62%
2½	50		26%		
	100		35%	36%	53%

The trend that is shown in Table 4 is that more energy is coupled into water for thinner pile walls, larger pile diameters, and higher explosive weights. These findings will be quantified more fully in the analysis and modeling section, which follows.

8.0 ANALYSIS AND MODEL DEVELOPMENT

The main result of the parametric numerical simulations was the determination of the amount of energy coupled to the water and, hence, the explosive coupling efficiency for the various pile scenarios (Table 4). The next step was to develop a model for the explosive coupling efficiency as a function of the pile attributes and the amount of explosive.

On the basis of thin-walled pressure vessel theory, in which the hoop stress is directly proportional to the internal pressure and radius (or diameter) and inversely proportional to wall thickness, we developed the pile parameter, p, as follows:

$$\text{Pile parameter,} \ \ p = \frac{w \cdot d}{t} \tag{1}$$

where: w = explosive weight, lbs.
d = pile diameter, inches
t = wall thickness, inches

We then plotted the explosive coupling efficiency versus the pile parameter, p, as shown in Figure 11. The data show that there is approximately a linear relationship to the three pile wall thicknesses that were studied. We fit a line to the points and came up with the following equation:

$$\text{Explosive coupling efficiency} \ (\%) = 34.37 + 0.005 \cdot p \ , \text{with} \ R^2 = 0.664 \tag{2}$$

There is some scatter in the results shown in Figure 11. This scatter is also indicated by the coefficient of determination (R^2) indicating that 66.4% of the uncertainty has been explained by the linear fit. The reason for this scatter is caused by the fact the piles were not severed to the same degree. Some walls were easily breached by the explosive while others did not fail as catastrophically. The pile parameter that we chose was just one of many possible. However, the form makes sense physically. More energy is coupled with increasing charge weight (the strength of the pile is over matched), increasing pile diameter (increased forces that the pile must resist), and decreasing wall thickness (higher stresses). As a side note, when the 1½-inch pile wall thickness results are plotted alone, a much better linear fit is obtained ($R^2 = 0.9134$) than when all the results are plotted together. The 1½-inch wall thickness data is banded more tightly and is more linear than the results for 2½-inch wall thickness numerical simulations. The lower coupling efficiencies for the 2½-inch wall thickness and lower explosive weight cases are caused by the increased pile confinement, which results in less catastrophic breaching.

The upper bound for the explosive coupling efficiency for 50 lbs of explosive buried 15 feet below the mud line should be approximately 80%, as that is the value for the clay only, no pile case (Table 3).

Having established the energy coupling factor for a particular pile configuration, the next step is to multiply the actual explosive charge weight by the explosive coupling efficiency and use the resulting reduced explosive weight to calculate the water shock using free-water methods. These

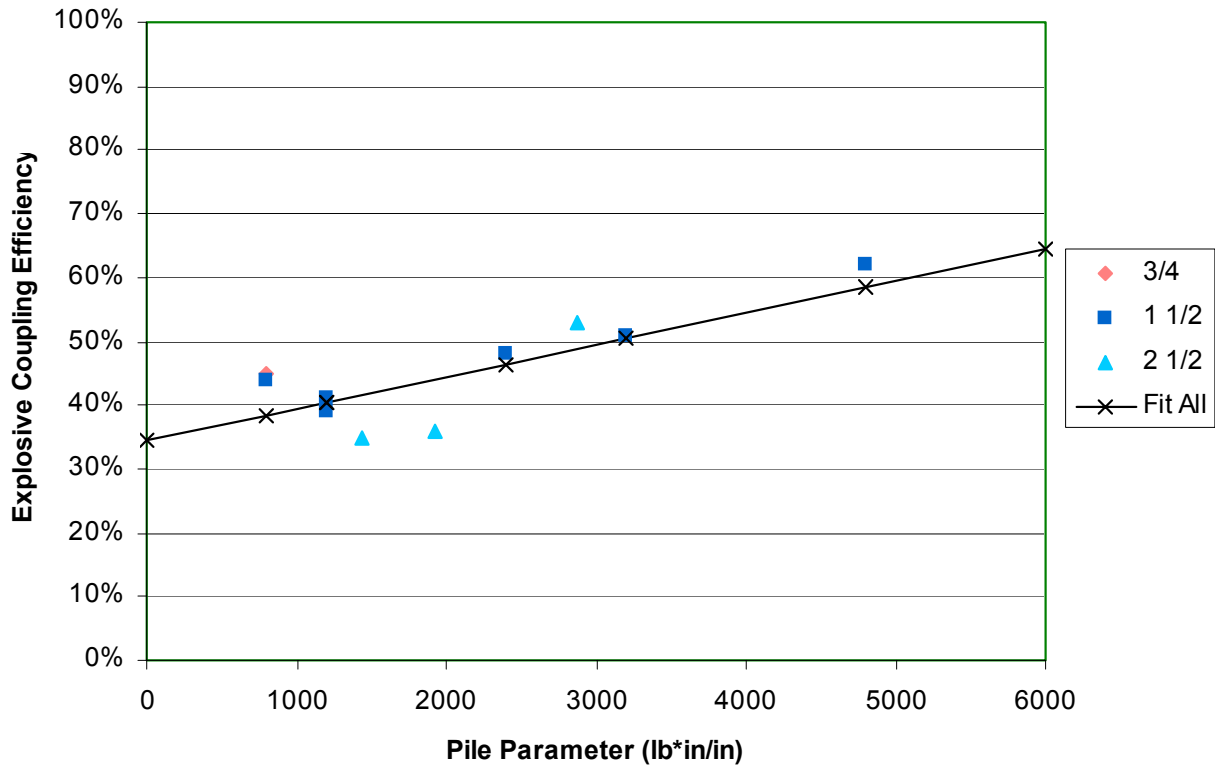methods are discussed in the next section and a spreadsheet calculator that we developed is described.

Figure 11. Relationship between the Explosive Coupling Efficiency and the Pile Parameter $\left(w \cdot \dfrac{d}{t} \right)$.

9.0 METHODS OF UNDERWATER SHOCK CALCULATION

This section describes the various ways the underwater shock event can be modeled for determining peak pressure, impulse, and energy flux density at range for an underwater explosion. Exploring these methodologies helped us better understand the limitations of each method. It is our goal to create a simple tool that offers accuracy and flexibility. However, "simple" means assumptions have been made and are applied to reduce the complexity and simplify use. The simplified tool is based on well-documented similitude equations and has been compared against other, more sophisticated methodologies, the most sophisticated of which is the computational continuum mechanics methodology. "Hydrocodes" such as CTH are numerical computational continuum mechanics tools that simulate the response of both solid and fluid material under such highly dynamic conditions (e.g., detonation and impact) that shock wave propagation is the dominant feature. The hydrocode approach to solving shock wave related problems makes few simplifying assumptions and thus offers the greatest complexity and greatest challenge to easy use. The other numerical method is the analytical wavecode. Analytical wavecodes such as REFMS (Britt et al., 1991) employ empirically derived relations and robust mathematical approximations to simulate the shock propagation environment. The analytical wavecode offers much less complexity than the hydrocode approach. Codes such as REFMS have been validated on a wide variety of underwater shock problems and used with much success. However, a significant level of sophistication to this method exists and limits the ease of use.

The comparison of the above described methods ensures that the simple tool is adequate for calculation purposes. The various methodologies will be further explained in the following sub-sections after discussion of some simplifying assumptions for all methods. The assumptions will allow all the methods to correlate.

9.1 Simplifying Assumptions for All Methods

Figure 12 shows the major wave types considered that affect pressure at a point in the water. The first wave in the water caused by a blast is the direct pressure wave or shock. The upper wave in Figure 12 shows its rapid rise and exponential-like decay. After some additional time there will be a rarefaction wave from the water-air interface. The reflection off the water-air interface is negative, caused by displacement of the surface. The air-water surface reflection is of nearly the same amplitude as the shock wave, because of the shock impedance mismatch with air. As shown in Figure 12, the air-surface reflection arrives later than the direct shock arrival because of the added distance traveled in reflection. The arrival time of the surface reflection depends upon geometric relationship of the explosive source, water-air interface, and the receiver.
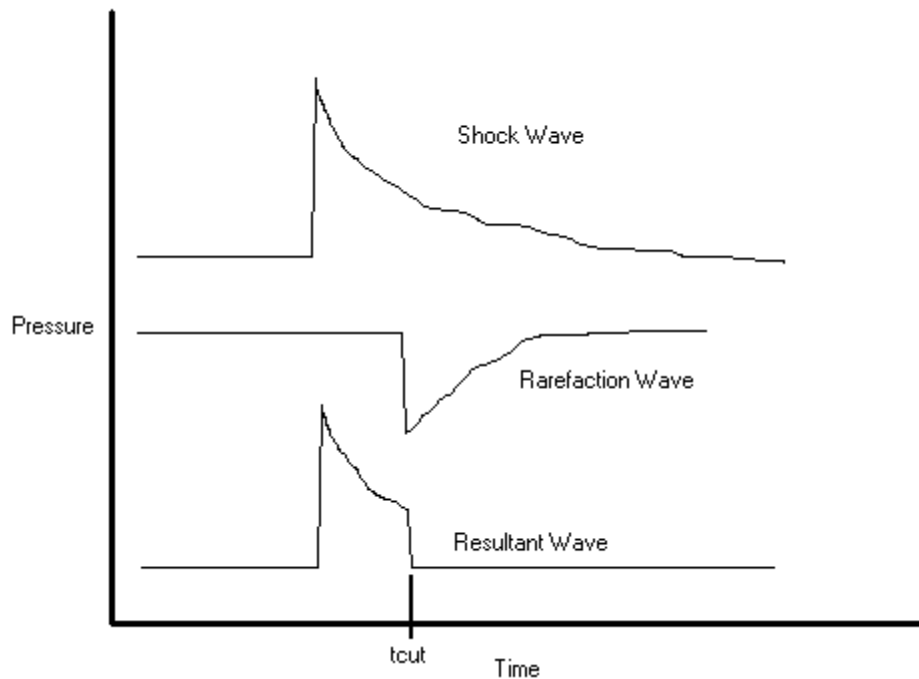
Figure 12. Superposition of Shock Waves.

The effects of the bottom surface, other structures, and other phenomena in and around the explosive source are not considered in this investigation. The bottom surface, however, is not a perfect reflector. The bottom surface absorbs shock energy. Typically, the amplitude of the wave reflected from the bottom surface is less than the direct shock wave. We are considering the amplitude of this wave to be in the same positive sense as the direct shock but much lower in value. Therefore, we are considering the bottom reflections as negligible for this study. The other shock interactions caused by the explosive event are much later in time. This study does not show possible multiple reflections between the air surface and the bottom, nor arriving bubble sphere peaks. We are only considering the shock interactions within the five or so time constants of the direct shock pulse.

9.2 Numerical – CTH Hydrocode

CTH is a first principle finite difference code that uses conservation of mass, momentum, and energy, along with equations-of-state and strength models to solve a defined explosive problem. This code was briefly described above in the Calculational Matrix Section (5.0). CTH is used to model the detonation and mechanical confinement of the explosive detonation products for an underwater pile configuration. The user has the ability to place sensors within the calculation to record pressures, impulse, and energy, as well as other parameters as a function of time at various ranges. The CTH is best suited to model the near field phenomena, i.e., the details of the explosive pile, clay, and water interaction. CTH was used in this study to understand the coupling of explosive energy into the water. On the basis of the results from CTH, we were able to develop an effective explosive yield for underwater pile explosions.

9.3 Similitude Equations - Spreadsheet Calculator

The pressure from an explosive detonation takes on a decreasing exponential form with respect to time. Depending on the distance from the blast, the pressure outside the explosive rises to a maximum pressure, Pm, in a very short time frame, usually that of several microseconds. The work of Cole (1948) and Swisdak et al. (1978) have demonstrated that the pressure as a function of time at some location from the explosive event will have the following form

$$P(t) = P_m e^{-(t/\theta)}$$

[3]

P_m is the initial maximum pressure and θ is the time constant. The time constant is the time over which the pressure-time history can be approximated with an exponential decay. Over practical ranges of interest, it has been empirically established that shock wave pressures decay at later times more slowly than that of an exponential decay (Swisdak et al., 1978). The pressure decline is closer to a linear decrease. The spreadsheet uses an exponential decay for the first 1.5 time constants of the pressure pulse, then a linear decay out to a calculated end time.

Swisdak et al. (1978) provide the equations for the parameters of the above pressure history equation [which are in metric units].

$$P_m = K \cdot (W^{1/3} / R)^{\alpha} \quad \text{(MPa)}$$

[4]

$$\theta = K_2 \cdot W^{1/3} (W^{1/3} / R)^{\alpha_2} \quad \text{(ms)}$$

[5]

The above equations use the slant distance, R, in meters, pressure in MPa, time in milliseconds (ms), and explosive weight in kilograms. The coefficients shown (K, K_2, α, and α_2) are specific to a given explosive. The inverse scaled range ($W^{1/3}/R$), the explosive weight divided by the slant range, is an important term. It allows the comparison of differing explosive weights. It provides the means to "scale" the pressure, energy, and effects on marine life from an underwater explosion. Equation [4] gives a good estimate of the pressure at distances from approximately 10 to 100 charge radii (Cole, 1948). The actual pressure in a given location can be affected by local conditions, such as water depth and bottom conditions. However, the bottom conditions are not considered in this study.

The effect of an underwater shock on marine life also depends on the time-integral of pressure (impulse), rather than the detailed form of the pressure-time history. The energy flux density is another significant measure of underwater shock. The energy flux density represents the energy flux across a unit area of a fixed surface normal to the direction of propagation of the wave (Cole, 1948). The impulse and energy flux density have the following forms:

$$I(t) = \int_0^\tau P(t) dt$$

[6]

$$E_f(t) = \frac{1}{\rho_o c_o} \cdot \int_0^{\tau} P^2(t)dt \qquad\qquad [7]$$

The integration interval τ is usually some multiplier of θ (typically $5*\theta$, Swisdak, et al., 1978) for I and E_f. The integration period should be determined by the purpose and intent of the explosive event. Others have documented that the integration period should be something on the order of $6.7*\theta$ (Cole, 1948). The multiplier on the time constant is a matter of choice based on the explosive event geometry. The integrals of equations [6] and [7] accurately resolve the strength and intensity of the shock wave at any point in the water continuum.

Often, the energy flux density is given in terms of decibels (dB) referenced to 1 μPa^2-s. The following two equations are the conversion relationships between the energy flux density in SI units and dB.

$$E_{dB} = 10 \cdot \log_{10}\left(\frac{E_f \cdot \rho_o c_o}{1 \cdot 10^{-12}}\right) \qquad\qquad [8]$$

Where: $\rho_o c_o$ = water impedance = 1.54 x 10^6 kg/(m^2 - s)

$$E_f = \frac{1 \cdot 10^{-12}}{\rho_o c_o} \cdot 10^{\frac{E_{dB}}{10}} \qquad\qquad [9]$$

All of the above relationships are for total energy flux density. Often the thresholds for affecting marine life are based on the value of energy flux density in any 1/3-octave band. Explosions are impulsive noise sources and are typically characterized by having a transient output signal. These transient signals contain a broadband of frequencies. To obtain the 1/3-octave band energy flux densities from a particular pressure time history requires a sophisticated analysis package. In lieu of this, we took the results from REFMS calculations for 50 lbs. of explosives and plotted the maximum 1/3-octave band energy flux density versus the total energy flux density (see Figure 13). The result was an approximate linear relationship between the two quantities that can be used to convert from one to the other. The coefficient of determination (R^2) was quite good (R^2 =0.94) for this relation. For example, a total EFD value of 192 dB yields a maximum 1/3-octave EFD of 181.6 dB. This is a reasonable result as for a broad band waveform, the 1/3-octave value is 10 dB lower than the total value.
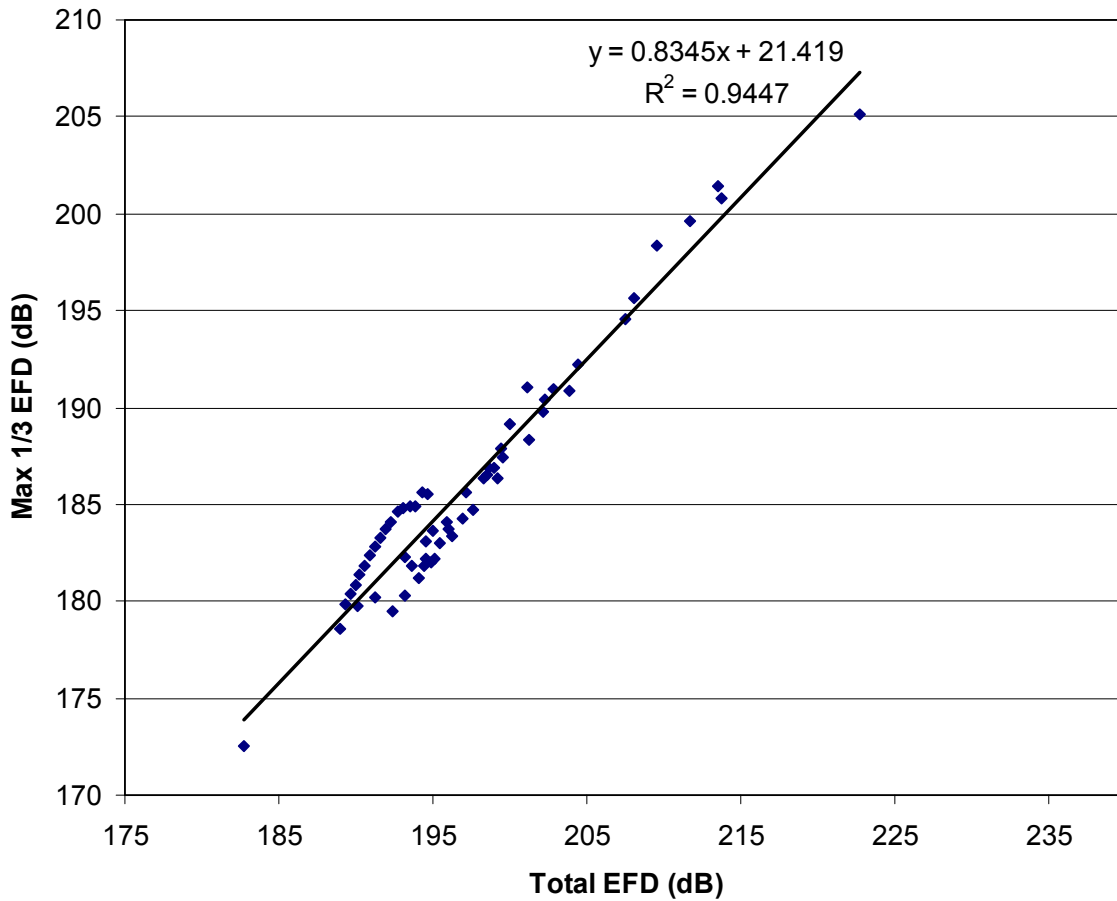
Figure 13. Relationship Between Maximum EFD in any 1/3-Octave Band and Total EFD.

The UnderWater Calculator (UWC) spreadsheet (Excel) performs both a forward calculation (input: slant range, output: pressure, impulse, EFD) and a backward calculation (input: peak pressure or EFD, output: slant range). The forward calculation includes the free surface effects while the backward calculation does not.

For the forward calculation, the spreadsheet takes into account surface rarefaction waves, which reduce the duration of the explosive shock pulse. The rarefaction wave interaction is based on where the explosive charge and receptor are located in relation to the water surface. Equation [10] provides the cut-off time. R' is the radial distance from the charge to the receptor the wave travels after being reflected from the surface. R is the slant range from the explosive to the receptor and c_o is the sound speed of the water.

$$t_{cut} = (R'-R)/c_o \qquad\qquad [10]$$

R' can be calculated from straightforward geometric relations resulting in Equation [11]. Sd is the source depth and Rd is the receptor depth from the water line. H is the horizontal range of

22

the receptor from the explosive charge.   Figure 14 illustrates the geometry for determining the cut-off time due to a surface rarefaction wave.

$$R' = \sqrt{(Sd + Rd)^2 + H^2}$$

[11]
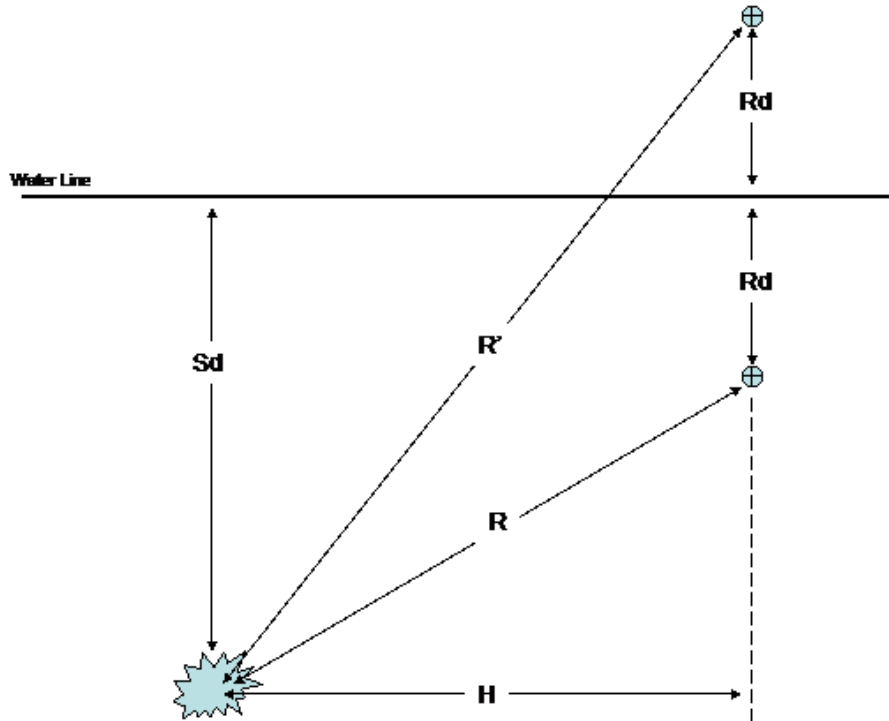
Figure 14. Geometry for Time Cut-Off of the Shock Pulse.

Figure 12 in the Simplifying Assumptions sub-section shows the end results of a shock pulse and rarefaction wave interaction. The cut-off time is calculated to determine the integration end time of the pressure time history. This allows for a more accurate computation of shock impulse and energy flux density.

9.4 Numerical – REFMS

REFMS v5.07 (Britt et al., 1991) is a computer program for predicting shock wave characteristics for explosions in water. It includes the aspects of near-source shock wave propagation caused by direct shock and water shock refraction from bottom and surface reflections. This code is designed to handle multi-layered ocean/bottom configurations with a variety of explosives sources available. The REFMS code has been extensively tested and validated against numerous high explosive experiments. It was used in the FEIS for the shock trials of the *Winston S. Churchill* (U.S. Dept. of the Navy, 2001). REFMS was used in that study to produce the pressure-time waveforms of shock wave transmission.

REFMS can be used to calculate peak pressures, pressure histories, impulse, and energy flux densities at a specified range. REFMS incorporates the Swisdak et al. (1978) shock formulations and closed-form ray-tracing analytical solutions to solve for the explosive shock environment.

However, the limiting factor of the REFMS code may be that it is quite sophisticated, allows very complex conditions, and the untrained user may have difficulty choosing the correct parameters for a particular calculation.

10.0 UNDERWATER CALCULATOR (UWC) SPREADSHEET EXAMPLES

This section presents examples using the UnderWater Calculator (UWC) spreadsheet, which is based upon the information given in Section 9.3. One free water calculation will be presented and compared with REFMS results. Then UWC results will be given to demonstrate the differences in range to effect for peak pressure and energy flux density between the free water and pile cases.

The free-water case is an open-water 22.68 kg (50 lb) H-6 explosive charge. The receiver is 400 meters from the surface and at a slant range of 403.11 meters. Given this geometry, the receptor is 50 meters horizontally from the source. The geometry of the free-water case is shown in Figure 15. The spreadsheet for this case is shown in Figure 16. Table 5 compares the UWC and REFMS results. The peak pressure, impulse and energy flux density are nearly the same for both methods.
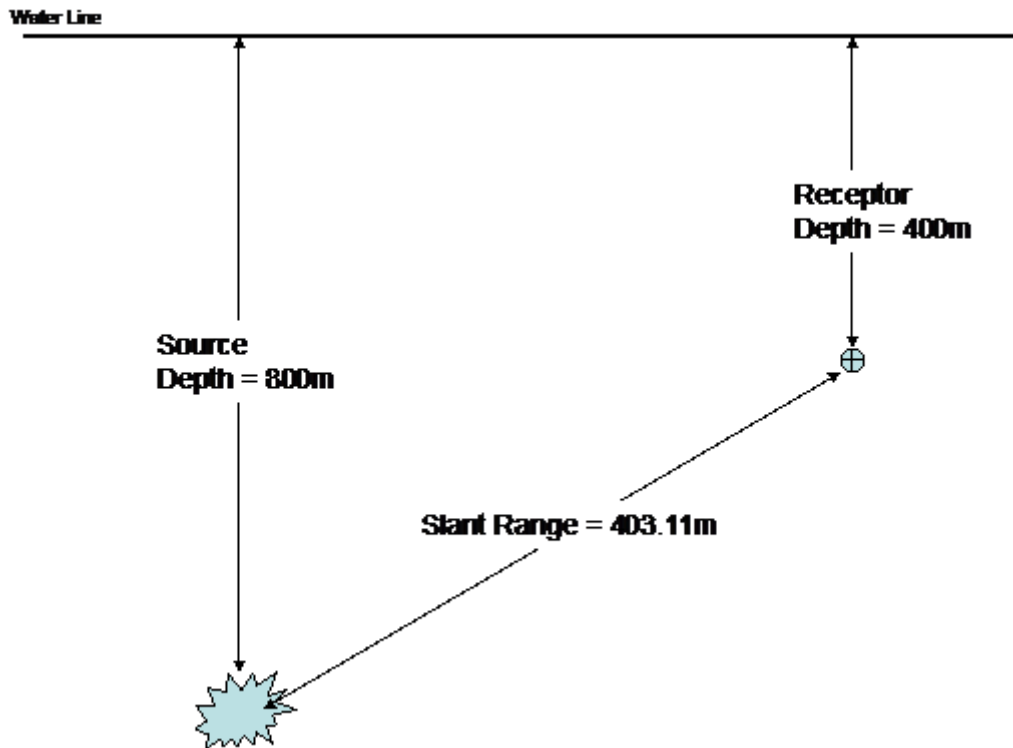

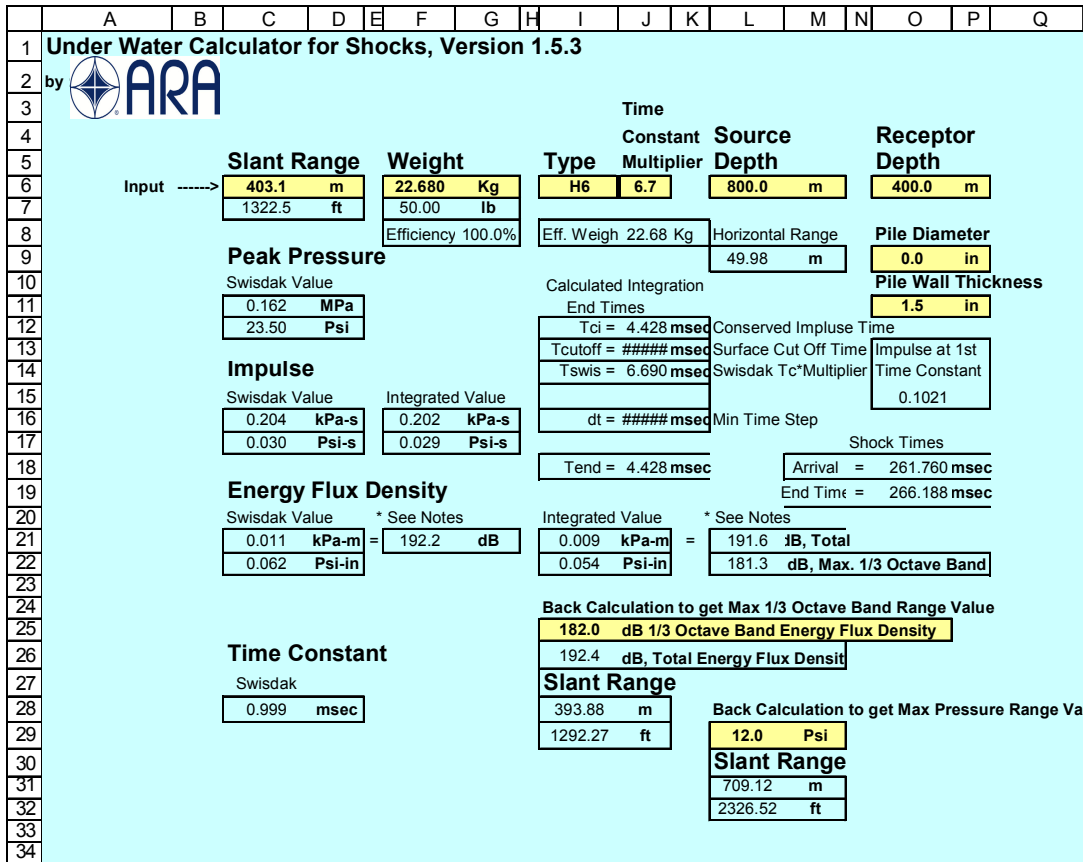Figure 15. Free-water Configuration Used for Comparison.

Under Water Calculator for Shocks, Version 1.5.3

by ◆ARA

	Slant Range	Weight	Type	Time Constant Multiplier	Source Depth	Receptor Depth
Input ------>	403.1 m	22.680 Kg	H6	6.7	800.0 m	400.0 m
	1322.5 ft	50.00 lb				
		Efficiency 100.0%	Eff. Weigh 22.68 Kg		Horizontal Range	Pile Diameter
	Peak Pressure				49.98 m	0.0 in
						Pile Wall Thickness
	Swisdak Value		Calculated Integration End Times			1.5 in
	0.162 MPa		Tci = 4.428 msec	Conserved Impluse Time		
	23.50 Psi		Tcutoff = #### msec	Surface Cut Off Time	Impulse at 1st
			Tswis = 6.690 msec	Swisdak Tc*Multiplier	Time Constant
	Impulse				0.1021
	Swisdak Value	Integrated Value	dt = #### msec	Min Time Step	
	0.204 kPa-s	0.202 kPa-s			
	0.030 Psi-s	0.029 Psi-s	Tend = 4.428 msec		Shock Times
					Arrival = 261.760 msec
	Energy Flux Density				End Time = 266.188 msec
	Swisdak Value	* See Notes	Integrated Value	* See Notes	
	0.011 kPa-m = 192.2 dB		0.009 kPa-m = 191.6 dB, Total		
	0.062 Psi-in		0.054 Psi-in	181.3 dB, Max. 1/3 Octave Band	
			Back Calculation to get Max 1/3 Octave Band Range Value		
			182.0 dB 1/3 Octave Band Energy Flux Density		
	Time Constant		192.4 dB, Total Energy Flux Densit		
	Swisdak		**Slant Range**		
	0.999 msec		393.88 m	**Back Calculation to get Max Pressure Range Va**	
			1292.27 ft	12.0 Psi	
				Slant Range	
				709.12 m	
				2326.52 ft	

Figure 16. UnderWater Calculator Spreadsheet for the Configuration in Figure 15.

Table 5. Results of the Free-water Case for the Two Methods.

Method	Peak Pressure (MPa)	Impulse (kPa-s)	Energy Flux Density re 1 $\mu Pa^2 s$ (dB)
REFMS	0.167	0.205	191.6
UWC	0.162	0.202	191.6

To demonstrate the difference in the shock propagation into the water between a free-water and a pile case, the UWC spreadsheet was exercised. The pile case is similar to the free-water case with the exception of the 36-inch diameter pile with a 1.5 inch wall thickness. The water depth was 200 meters and the receiver depth was 100 meters. We performed a series of calculations to determine the range for a given energy flux density (182 dB for any 1/3-octave band) and for a given peak pressure (12 psi). The results for the free-water charge and the buried pile charge are shown in Tables 6 and 7. As can be seen from these two tables, the range to effect for the pile case is less than the free-water case. This is an expected result because of the reduced energy coupling to the water for the pile configuration.

Table 6. 50-lb H-6 Charge, Range to 182-dB Energy Flux Density.

Explosive Configuration	Range (m)	Peak Pressure (psi)	Total Energy Flux Density re 1 μPa^2s (dB)	Max 1/3 Octave Band Energy Flux Density re 1 μPa^2s (dB)
Free-Water Charge	394	24.2	191.8	181.5
Buried Pile Charge	252	28.7	191.8	181.5

Table 7. 50-lb H-6 Charge, Range to 12-psi Peak Pressure.

Explosive Configuration	Range (m)	Peak Pressure (psi)	Total Energy Flux Density re 1 μPa^2s (dB)	Max 1/3 Octave Band Energy Flux Density re 1 μPa^2s (dB)
Free-Water Charge	710	11.98	186.5	177.0
Buried Pile Charge	525	11.98	185.1	175.9

In order to minimize the effect on marine mammals and other aquatic life, the dual criteria of 12 psi (acceptable peak pressure level) and 182 dB re 1 μPa^2s (acceptable received energy density level in any 1/3-octave band) to define the impact zone radius are cited by the National Oceanic and Atmospheric Administration (NOAA) Fisheries Service. Tables 6 and 7 illustrate the difference of range to effect between the two criteria. As indicated by the UWC tool in the above tables, the energy criteria provides approximately a 50% smaller slant range than the peak pressure criteria. The Churchill shock trials FEIS (U.S. Dept. of the Navy, 2001) indicates that the 182-dB energy criterion was more frequently the determining factor in defining the impact zone radius (10,000 lb explosive charge). The determining factor as to which criterion governs is based on the explosive charge weight. For smaller charge weights, the pressure criterion will govern (Tables 6 and 7), while for larger charges, the energy flux density criterion will govern (Churchill shock trials). The crossover point is approximately 2,000 lbs; i.e., below 2,000 lbs, the pressure criterion will yield the greater impact zone radius, while above 2,000 lbs, the energy flux density criterion will determine the impact zone radius.

11.0 SUMMARY

The objective of this work was to develop a method to determine the shock wave propagation into water caused by the removal of offshore structures by explosive methods. This was accomplished by performing numerical simulations of various explosive, pile, clay, water systems and determining the amount of energy coupled to the water. The numerical simulations showed that less energy is coupled to the water for the pile cases than would be coupled for free water explosions. These simulations showed that a reduction of coupled energy into the water was dominated by pile confinement followed by soil confinement. Parametric numerical simulations were performed that covered a range of typical pile diameters, wall thicknesses, and explosive weight. From these results, a model was developed to predict the explosive efficiency factors for various pile scenarios. Lastly, the UnderWater Calculator spreadsheet was developed to predict peak pressure, impulse, and energy flux density for both the free-water and pile cases.

12.0 RECOMMENDATIONS

The model development and the UnderWater Calculator are based on the numerical simulations for a fairly wide range of parameters (Section 4.0). A natural extension for the model would be to extend the explosive coupling efficiency/pile parameter relation to include the pile steel yield strength, explosive depth of burial, and more complex structures (e.g., the inclusion of grout). The UnderWater Calculator should be evaluated for shallow water conditions and modified if necessary. Lastly, the model results should continually be compared to existing data from EROS operations.

13.0 REFERENCES

Britt, J.R., R.J. Eubanks, and M.G. Lumsden. 1991. Underwater shock wave reflection and refraction in deep and shallow water: Volume I - A User's Manual for the REFMS Code (Version 4.0). Science Applications International Corporation, St. Joseph, LA. DNR-TR-91-15-VI.

Cole, R.H. 1948. Underwater explosions. Princeton: Princeton University Press.

Connor, Jr., J.G. 1990. Underwater blast effects from explosive severance of offshore platform legs and well conductors. Naval Surface Warfare Center, Silver Spring, MD. NAVSWC TR 90-532. 34 pp.

Goertner, J.F. 1982. Prediction of underwater explosion safe ranges for sea mammals. Naval Surface Weapons Center, Silver Spring, MD. NSWC TR 82-188. 25 pp.

Mader, C.S. 1979. Numerical modeling of detonations (Los Alamos series in basic and applied science). Berkeley: University of California Press.

McGlaun, J.M., S.L. Thompson, M.G. Elrick. 1990. CTH: A three-dimensional shock wave physics code. Int. J. Impact Engng. 10: 351-360.

Richardson, W.J., C.R. Greene Jr., C.I. Malme, and D.H. Thomson. 1995. Marine mammals and noise. San Diego: Academic Press. 576 pp.

Swisdak, Jr., M.M. 1978. Explosion effects and properties: Part II - Explosion effects in water. Naval Surface Weapons Center, Silver Spring, MD. NSWC/WOL TR 76-116.

U.S. Department of the Navy. 2001. Final environmental impact statement: Shock trial of the *Winston S. Churchill* (DDG81). Southern Division, Naval Facilities Engineering Command, North Charleston, SC. 229 pp. + appendices.

Ward, P.D., M.K. Donnelly, A.D. Heathershaw, S.G. Marks, and S.A. Jones. 1998. Assessing the impact of underwater sound on marine mammals. In: Tasker, M.L. and C. Weir, eds. Proceedings of the Seismic and Marine Mammals Workshop, June 23-25, London, England.

Yelverton, J.T., D.R. Richmond, E.R. Fletcher, and R.K. Jones. 1973. Safe distances from underwater explosions for mammals and birds. Report by the Lovelace Foundation for Medical Education and Research, Albuquerque, NM, for Defense Nuclear Agency, Washington, DC. Technical Report No. 3114 T. 72 pp.

Young, G.A. 1991. Concise methods for predicting the effects of underwater explosions on marine life. Naval Surface Warfare Center, Silver Spring, MD. NAVSWC MP 91-220. 22 pp.

APPENDIX A

BIBLIOGRAPHY

BIBLIOGRAPHY

Al-Hassani, S.T.S. 1988. Explosive cutting techniques for offshore applications. Manchester: Thomas Telford, Ltd.

Al-Hassani, S.T.S. 1988. Platform removal demands complex explosive designs. Oil and Gas Journal, 86(20): 35-38.

BP Exploration (Alaska) Inc. 2001. Technical Brief: Alaska's North Slope Oilfields: Bowhead whales (Balaena mysticetus). Internet website: http://alaska.bp.com/alaska/environment/EnvStudies/pdf/3MAMMALS/gBowhead_Whales.pdf.

Britt, J.R., R.J. Eubanks, and M.G. Lumsden. 1991. Underwater shock wave reflection and refraction in deep and shallow water: Volume I - A User's Manual for the REFMS Code (Version 4.0). Science Applications International Corporation, St. Joseph, LA. DNR-TR-91-15-VI.

Cole, R.H. 1948. Underwater explosions. Princeton: Princeton University Press.

Connor, Jr., J.G. 1990. Underwater blast effects from explosive severance of offshore platform legs and well conductors. Naval Surface Warfare Center, Silver Spring, MD. NAVSWC TR 90-532. 34 pp.

Digges, T. 1990. The practical use of explosives for abandonment and removal of offshore structures. London: Thomas Telford, Ltd.

Edbon, R., R. Surle, and P. Minardi. 1990. A multi-disciplinary European approach to developing technologies for the removal of offshore platforms. London: Graham and Trotman, Ltd.

Finneran, J.J., C.E. Schlundt, D.A. Carder, J.A. Clark, J.A. Young, J.B. Gaspin, and S.H. Ridgway. 2000. Auditory and behavioral responses of bottlenose dolphins (*Tursiops truncatus*) and a beluga whale (*Delphinapterus leucas*) to impulsive sounds resembling distant signatures of underwater explosions. Journal of the Acoustical Society of America. 108(1): 417-431.

Gitschlag, G.R. 1997. Fisheries impacts of underwater explosives used to salvage oil and gas platforms in the Gulf of Mexico. In: Proceedings of the 23rd annual conference on explosives and blasting technique. Cleveland: International Society of Explosives Engineers. 667 pp.

Goertner, J.F. 1982. Prediction of underwater explosion safe ranges for sea mammals. Naval Surface Weapons Center, Silver Spring, MD. NSWC TR 82-188. 25 pp.

Lynch, R.T., L.R. Settle, J.J. Govoni, M.D. Green, M.A. West, and G. Revy. 2001. Instrumentation report for the preliminary investigation of underwater explosions on larval and early juvenile fishes. Final Report by Applied Research Associates, Inc. for the U.S. Army Corps of Engineers Wilmington District, Wilmington, NC. Project No. 0540.

Mader, C.S. 1979. Numerical modeling of detonations (Los Alamos series in basic and applied science). Berkeley: University of California Press.

Maeda, H., K. Ito, T. Shindo, F. Takeishi, and T. Kano. 1993. Pile and conductor cutting with explosives of oil drilling platform removal at Offshore Niigata Prefecture, Japan, Part 1. Journal of the Industrial Explosives Society. 54(6): 310-315.

McGlaun, J.M., S.L. Thompson, and M.G. Elrick. 1990. CTH: A three-dimensional shock wave physics code. Int. J. Impact Engng. 10: 351-360.

Pulsipher, A.G. (ed.). 1996. Proceedings: An international workshop on offshore lease Abandonment and platform disposal: Technology, regulation, and environmental effects, April 15-17, 1996. Center for Energy Studies, Louisiana State University, Baton Rouge, LA. MMS Contract 14-35-0001-30794. 312 pp.

Pulsipher, A., W. Daniel IV, J.E. Kiesler, and V. Mackey III. 1996. Explosives remain preferred methods for platform abandonment. Oil and Gas Journal. 94(19): 64-70.

Richardson, W.J., C.R. Greene Jr., C.I. Malme, and D.H. Thomson. 1995. Marine mammals and noise. San Diego: Academic Press. 576 pp.

Ridgway, S.H., D.A. Carder, R.R. Smith, T. Kamolnick, C.E. Schlundt, and W.R. Elsberry. 1997. Behavioral responses and temporary shift in masked hearing threshold of Bottlenose dolphins (*Tursiops truncatus*) to 1-second tones of 141 to 201 dB re 1 μPa. Naval Command, Control and Ocean Surveillance Center, San Diego, CA. TR 175-1.

Simple measures reduce marine mammal injuries during platform removal. 1994. Oil and Gas Journal. 92(37): 89-90.

Swisdak, Jr., M.M. 1978. Explosion effects and properties: Part II - Explosion effects in water. Naval Surface Weapons Center, Silver Spring, MD. NSWC/WOL TR 76-116.

Takahashi, K., K. Murata, A. Torii, and Y. Kato. 2002. Enhancement of underwater shock wave by metal confinement. In: Technical Papers of the 12th International Detonation Symposium, August 11-16, San Diego, CA. Pp. 466-474.

Thornton, W.L. 1989. Case history. In: Proceedings of the 21st annual offshore technology Conference. Houston: Offshore Technology Conference. Pp. 295-304.

U.S. Department of Commerce, National Oceanic and Atmospheric Administration. 2001. Taking and improving marine mammals; taking marine mammals incidental to native activities. 50 CFR Part 216, *Federal Register*, Vol. 66, No. 87. May 4, 2001.

U.S. Department of the Navy. 2001. Final environmental impact statement: Shock trial of the *Winston S. Churchill* (DDG81). Southern Division, Naval Facilities Engineering Command, North Charleston, SC. 229 pp. + appendices.

Ward, P.D., M.K. Donnelly, A.D. Heathershaw, S.G. Marks, and S.A. Jones. 1998. Assessing the impact of underwater sound on marine mammals. In: Tasker, M.L. and C. Weir, eds. Proceedings of the Seismic and Marine Mammals Workshop, June 23-25, London, England.

Whyte, I.L. 1988. Decommissioning – 1988. In: International conference on decommissioning offshore, onshore and nuclear works. London: Thomas Telford, Ltd. 342 pp.

Yelverton, J.T., D.R. Richmond, E.R. Fletcher, and R.K. Jones. 1973. Safe distances from underwater explosions for mammals and birds. Report by the Lovelace Foundation for Medical Education and Research, Albuquerque, NM, for Defense Nuclear Agency, Washington, DC. Technical Report No. 3114 T. 72 pp.

Young, G.A. 1991. Concise methods for predicting the effects of underwater explosions on marine life. Naval Surface Warfare Center, Silver Spring, MD. NAVSWC MP 91-220. 22 pp.

The Department of the Interior Mission

As the Nation's principal conservation agency, the Department of the Interior has responsibility for most of our nationally owned public lands and natural resources. This includes fostering sound use of our land and water resources; protecting our fish, wildlife, and biological diversity; preserving the environmental and cultural values of our national parks and historical places; and providing for the enjoyment of life through outdoor recreation. The Department assesses our energy and mineral resources and works to ensure that their development is in the best interests of all our people by encouraging stewardship and citizen participation in their care. The Department also has a major responsibility for American Indian reservation communities and for people who live in island territories under U.S. administration.

The Minerals Management Service Mission

As a bureau of the Department of the Interior, the Minerals Management Service's (MMS) primary responsibilities are to manage the mineral resources located on the Nation's Outer Continental Shelf (OCS), collect revenue from the Federal OCS and onshore Federal and Indian lands, and distribute those revenues.

Moreover, in working to meet its responsibilities, the **Offshore Minerals Management Program** administers the OCS competitive leasing program and oversees the safe and environmentally sound exploration and production of our Nation's offshore natural gas, oil and other mineral resources. The MMS **Minerals Revenue Management** meets its responsibilities by ensuring the efficient, timely and accurate collection and disbursement of revenue from mineral leasing and production due to Indian tribes and allottees, States and the U.S. Treasury.

The MMS strives to fulfill its responsibilities through the general guiding principles of: (1) being responsive to the public's concerns and interests by maintaining a dialogue with all potentially affected parties and (2) carrying out its programs with an emphasis on working to enhance the quality of life for all Americans by lending MMS assistance and expertise to economic development and environmental protection.